Journal of Alloys and Compounds 509 (2011) 4439–4444

Contents lists available at ScienceDirect

Journal of Alloys and Compounds

journal homepage: www.elsevier.com/locate/jallcom

Thermodynamic assessment of Au–La and Au–Er binary systems

H.Q. Dong[a,*], X.M. Tao[b], H.S. Liu[c], T. Laurila[a], M. Paulastro-Kröckel[a]

[a] Department of Electronics, Aalto University School of Science and Technology, FIN-02601 Espoo, Finland
[b] Key Laboratory of New Processing Technology for Nonferrous Metals and Materials of Ministry of Education, Department of Physics, Guangxi University, Nanning 530004, PR China
[c] The Scientific Center of Phase Diagrams & Materials Design, Central South University, Changsha, Hunan 410083, PR China

ARTICLE INFO

Article history:
Received 13 November 2010
Accepted 9 January 2011
Available online 14 January 2011

Keywords:
Au–La
Au–Er
CALPHAD
Thermodynamic assessment
Ab initio calculations

ABSTRACT

Phase relationships in Au–La and Au–Er binary systems have been thermodynamically assessed by using the CALPHAD technique. The existing thermodynamic descriptions of the systems were improved by incorporating the ab initio calculated enthalpies of formation of the intermetallic compounds, except for the $Au_{51}La_{14}$ and $Au_{10}Er_7$ phases. All the binary intermetallic compounds were treated as stoichiometric phases, while the solution phases, including liquid, fcc, bcc, and dhcp, were treated as substitutional solution phases and the excess Gibbs energies were formulated with Redlich–Kister polynomial function. As a result, two self-consist thermodynamic data sets for describing the Au–La and Au–Er binary systems were obtained.

1. Introduction

The eutectic Au–20 wt.% Sn solder is broadly used in electronic industries due to its excellent fatigue and creep resistances as well as because of the possibility of fluxless bonding process [1]. Owing to the scarce resources and high price of Au as well as due to the poor mechanical properties of the Au–Sn intermetallic compounds, materials to replace Au or at least to reduce its use are constantly searched for.

During the recent years most of the attention with this respect has been focused on the rare earth elements (RE), as they can refine the mechanical properties and improve the wettability of solders. Moreover, RE can, by reducing the oxidization of solder and by cleaning the grain boundaries, improve the fatigue performance under slow deformation [2–4]. Despite the major interest towards RE elements, there exists practically no reported research about the effect of rare earth elements on the thermodynamic properties of Au–Sn solder. As the development of the phase diagram of Au–Sn–RE systems is of central importance when choosing the composition of a new solder as well as for understanding the materials compatibility between the chosen solder and different metallizations used, there is a clear need for further thermodynamic investigations on the Au–Sn–RE systems.

Unfortunately, the description of both Au–RE and Sn–RE systems is presently inadequate, let alone the Au–Sn–RE ternary system. Thus, in the present work, the Au–La and Au–Er binary systems were chosen for critical assessment, since both of them have been recently studied experimentally and further there exists certain confusion about the invariable reactions occurring in the systems, two in Au–La [5] and one in Au–Er [6].

Hence, the purpose of the present work is to critically assess the Au–La and Au–Er binary systems and to develop a precise thermodynamic description by means of the CALculation of PHAse Diagram (CALPHAD) technique [7] combined with the ab initio methods [8,9].

2. Evaluation of the available information

2.1. The Au–La binary system

The equilibrium phase diagram of Au–La was experimentally determined already in 1931 [10]. In 1965 the quite small solubility range of lanthanum in gold (i.e. 0.1 at.%) was determined by Rider et al. [11] using the X-ray parametric method. In 1971, McMasters et al. [12] investigated and reviewed the crystal structures of the intermetallic compounds in lanthanide–gold system, by means of powder and single-crystal X-ray diffraction. Later, Steeb et al. [13] carried out some further research about the crystal structures of intermetallic compounds. Regarding this, it is to be noted that a different prototype for the stoichiometric phase Au_6RE was used in Refs. [12,13], i.e. Au_6Pr and Au_6Ce, respectively. In 1974, Moreau and Parthe [14] conducted further investigations to resolve the second crystal structure and to elucidate the structural features common to these two new structure types. The outcome of the

* Corresponding author.
E-mail address: hongqun.dong@aalto.fi (H.Q. Dong).

0925-8388/$ – see front matter © 2011 Elsevier B.V. All rights reserved.
doi:10.1016/j.jallcom.2011.01.072

study was to confirm Au_6Pr as the correct prototype for Au_6RE compound. One year later, Johnson and Duwez [15] studied the amorphous superconducting Au–La alloys of the form Au_xLa_{100-x}, where x ranged from 0 to 40 at.% obtained by liquid quenching. The phase diagram of Au–La has not been further investigated since Massalshi et al. [5] assessed it based on the data from Refs. [10,12–14]. In this assessment the uncertainty regarding the existence of the Au_6La phase was not solved. Based on the knowledge about the other Au–rare earth binary systems [5], it is known that if there occurs a $Au_{51}RE_{14}$ compound in a given system, also the existence of the Au_6RE compound in that binary system is expected. In the present work, the temperatures of the two invariable reactions involved in the system under investigation are compared to those occurring in other Au–RE systems to check the consistency of the results.

Regarding the thermochemical data, the enthalpies of mixing in the binary system at 1473 ± 2 K have been measured by employing high-temperature reaction calorimetry method by Fitzner et al. [16]. What comes to the standard enthalpies of formation of the intermetallic compounds, only that of $Au_{51}La_{14}$ [17] phase has been determined. Thus, more thermochemical information is clearly needed. In the present work, the ab initio approach has been utilized to calculate the enthalpies of formation of the intermetallic compounds in the Au–La binary system. Subsequently, the thermodynamic reassessment of the Au–La system was carried out.

2.2. The Au–Er binary system

In 1965, Rider et al. [11] determined the solid solubilities of rare earth element Er in gold by X-ray parametric method. With the similar method (i.e. X-ray powder diffractometry), in 1968, Sadagopan et al. [18] investigated the binary alloy phases in the Au–Er system covering the concentration range between Au_2Er and Au. The crystal structures of the Au_2Er and Au_4Er phases were also determined in this investigation. Later, in 1971, McMasters et al. [12] reported the crystal structures of the intermetallic compounds in the Au–Er system, except for that of $Au_{10}Er_7$ and further established the melting point of AuEr as 1983 ± 10 K. In addition, they made a statement about the existence of the βAuEr $\leftrightarrow$ αAuEr transition, even though the transition temperature was not explicitly measured. Then, in 1987 Massalski et al. [5] calculated the phase diagram of this system by assuming the liquid to be a subregular solution and the solid phases to be line compounds. There was no further investigation of the phase diagram of the Au–Er binary system until 2002 Saccone et al. [6] experimentally reestablished the phase diagram of this system in, by means of power X-ray diffraction, optical and scanning microscopy, electron probe microanalysis and differential thermal analysis. In addition, a new compound $Au_{10}Er_7$ and four eutectic reactions involving $AuEr_2$, Au_2Er and Au_3Er phases were found in [6] In the present work, the phase diagram information is based in Ref. [6].

As for the thermochemical information, no enthalpies of mixing have been reported in the system. In 2000 the activity of Er through out the Au–Er system between 973 K and 1073 K was determined, by using e.m.f. technique and employing CaF_2 as the solid electrolyte [19]. Later, in 2004 Meschel and Kleppa [17] measured the standard enthalpies of formation of AuEr, Au_2Er and Au_3Er phases by high temperature direct synthesis calorimetry at 1373 K. Recently, in 2006 Wu et al. [20] calculated the enthalpies of formation of the intermetallic compounds of the Au–Er system, except that of the $Au_{10}Er_7$ phase, by VASP software. In the report the enthalpy of formation of αAuEr (low temperature form) is more positive than that of βAuEr (high temperature form), which cannot be correct. In fact based on the thermodynamic stability theory, the enthalpy of formation of the low temperature phase in a allotropic transformation should always be more negative than that of the high temperature phase. Therefore, these enthalpies were recalculated by the ab initio method in the present work.

3. Calculation method

3.1. Ab initio calculations

In order to get the lattice stability of metastable Er(fcc) and the enthalpies of formation of the intermetallic compounds of the Au–La and Au-Er system, an ab initio approach was performed by using the scalar relativistic all-electron Blöchl's projector augmented-wave (PAW) method [21,22] within the generalized gradient approximation (GGA), as implemented in the highly-efficient Vienna ab initio simulation package (VASP) [8,9]. For the GGA exchange-correlation function, the Perdew–Wang parameterization (PW91) [23,24] was employed. A constant plane-wave energy cutoff of 450 eV was used for the A_xB_y compounds. Brillouin-zone integrations were performed using Monkhorst-Pack [25] K-point meshes, and the Methfessel–Paxton [26] technique with the smearing parameter of 0.2 eV. The reciprocal space (k-point) meshes were increased to achieve convergence to a precision of 5 meV/atom. The total energy converged numerically to less than 1×10^{-6} eV/unit with respect to electronic, ionic and unit cell degrees of freedom, and the latter two were relaxed using Hellman–Feymann forces with a preconditioned conjugated gradient algorithm. After structural optimization, the Hellman–Feymann forces on each ion were less than 0.01 eV/Å. All calculations were performed using the "high" setting within VASP to avoid wrap-around errors. In addition, spin polarization was used in all calculations.

The enthalpies of formation of the IMCs were calculated by the following equation

$$\Delta H(A_xB_y) = E_{\text{total}}(A_xB_y) - xE_{\text{total}}(A) - yE_{\text{total}}(B) \quad (1)$$

where $E_{\text{total}}(A_xB_y)$, $E_{\text{total}}(A)$, and $E_{\text{total}}(B)$ are the calculated total energies (per atom at $T = 0$ K) of the IMCs for pure A and B, respectively.

3.2. Thermodynamic models

The lattice stability of the element i(i = Au, La and Er, except for Er(fcc)) is referred to the constant enthalpy value of the so-called standard element reference H_i^{SER} at 298.15 K and 1 bar as recommended by SGTE (Scientific Group Thermodata Europe), compiled in the paper by Dinsdale [27]. As for the lattice stability of Er(fcc), it was calculated by ab initio approach in this work. Different models were employed to describe the solution phases and IMCs of the Au–ER binary systems (RE = La and Er).

3.2.1. Solution phases: liquid, Au(fcc) and Er(hcp)

An ordinary substitutional solution model was applied to depict the liquid, fcc and hcp terminal solutions. The molar Gibbs energy of a solution phase Φ (Φ = liquid, fcc, hcp, bcc) can be represented as a sum of the Gibbs energy for the pure components, the ideal entropy term describing a random mixing of the components, and the excess Gibbs energy describing the deviation from ideal mixing, i.e.

$$G^{\phi} = \sum_{i=\text{Au, RE,}} x_i {}^0G_i^{\phi} + RT \sum_{i=\text{Au, RE}} x_i \ln(x_i) + {}^{ex}G^{\phi} \quad (2)$$

where R is the gas constant, T is the temperature in Kelvin, x_i is the molar fraction of component i(=Au, RE), and ${}^0G_i^{\phi}$ is the molar Gibbs energy of pure element i, with the crystal structure of ϕ. And the

Table 1
Enthalpies of formation at 0 K obtained by an *Ab Initio* calculation and the other one's work at 298 K. Reference. states: Au(fcc), La(dhcp) and Er(hcp).

Phase	Prototype	This work, ab initio (kJ/mol)	Wu, VASP (kJ/mol)	Meschel (±1.9) (kJ/mol)	Alqasmi	Lattice parameters (pm)		
						a	*b*	*c*
$AuLa_2$	Co_2Si [12]	−56.6	–	–	–	739.7	5.107	941.0
αAuLa	FeB [12]	−82.0	–	–	–	752.0	469.0	596.0
βAuLa	CrB [12]	−82.5	–	–	–	395.0	1120	478.0
Au_2La	$CeCu_2$ [12]	−81.5	–	–	–	470.0	729.5	815.5
$Au_{51}La_{14}$	$Gd_{14}Ag_{51}$ [12]	–	–	−57.9	–	1287		938.8
$AuLa_6$	Au_6Pr [12]	−45.1	–	–	–	–	–	–
$AuEr_2$	Co_2Si [12]	−67.0	−52.2	–	–	699.6	486.9	880.2
αAuEr	CrB [12]	−90.9	−77.0	−90.2	–	365.0	1081	458.0
βAuEr	CsCl [12]	−88.6	−87.7	–	−85.1	353.5		
$Au_{10}Er_7$	Gd_7Au_{10} [6]	–	–	–	–	1017		2763
Au_2Er	$MoSi_2$ [18]	−88.4	−86.0	−85.9	−79.0	366.3		891.6
Au_3Er	Cu_3Ti [18]	−73.0	−71.1	−66.1	−65.9	602.9	494.9	507.9
Au_4Er	$MoNi_4$ [18]	−60.3	−59.2	–	–	663.6		414.9

excess term is formulated as

$$^{ex}G^{\phi} = x_{Au}x_{RE}\sum_{j=0,1\ldots}^{N} {}^{(j)}L^{\phi}_{Au,RE}(x_{Au}-x_{RE})^{j} \quad (3)$$

where $^{(j)}L^{\phi}_{Au,RE}$ is the interaction parameter between Au and ER elements, which were taken to be temperature dependent:

$$^{(j)}L^{\phi} = a + bT + cT\ln T + dT^2 + eT^3 + fT^{-1} \quad (4)$$

where parameters a and b were to be optimized.

3.2.2. Stoichiometric intermetallic phases

No significant solubilities of the solid phases has been reported [5,12] and therefore all the intermetallic phases, total of 6 in the Au–La binary system and 7 in Au–Er binary system, were treated as line compounds. The Gibbs energy per mole of formula unit Au_mRE_n is expressed as

$$G^{Au_mRE_n} = m\,GH^{SER}_{Au} + n\,GH^{SER}_{RE} + \Delta G_f^{Au_mRE_n} \quad (5)$$

where $\Delta G_f^{Au_mRE_n}$ is the Gibbs energy of formation of per mole of formula unit of the Au_mRE_n. Due to lack of experimental measurements, it is assumed that the Neumann–Kopp rule applies to the heat capacity, i.e. $\Delta G_p = 0$. Thus the $\Delta G_f^{Au_mRE_n}$ can be expressed as

$$\Delta G_f^{Au_mRE_n} = A + BT \quad (6)$$

with *A* and *B* to be assessed in the present work.

4. Results and discussion

4.1. Ab initio calculations

Due to the insufficiency of the thermodynamic data, the ab initio method was employed to calculate the enthalpies of formation of the intermetallic compounds in the Au–RE (RE = La and Er) systems. In addition the lattice stability of metastable Er(fcc) was calculated in this work. As shown in Table 1, the results of the ab initio approach in the present work are in good agreement with the experimental outcomes and others' calculated data, since all the deviation are less than 5%. Due to the inconsistency of the data from Ref. [20], as discussed in Section 2.2, the data from this work were not employed during optimization. The initial data for the thermodynamic parameters of these compounds were adopted based on the ab initio calculated data in the present work. In addition, these data were illustrated in Figs. 1 and 2.

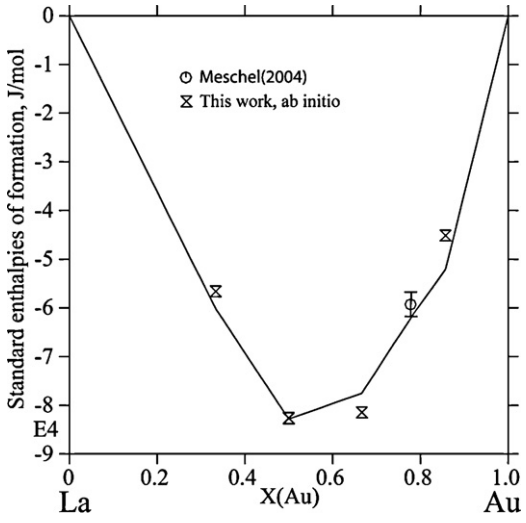

Fig. 1. Enthalpies of formation in the Au–La binary system at 298 K. Reference states: Au(fcc) and La(dhcp).

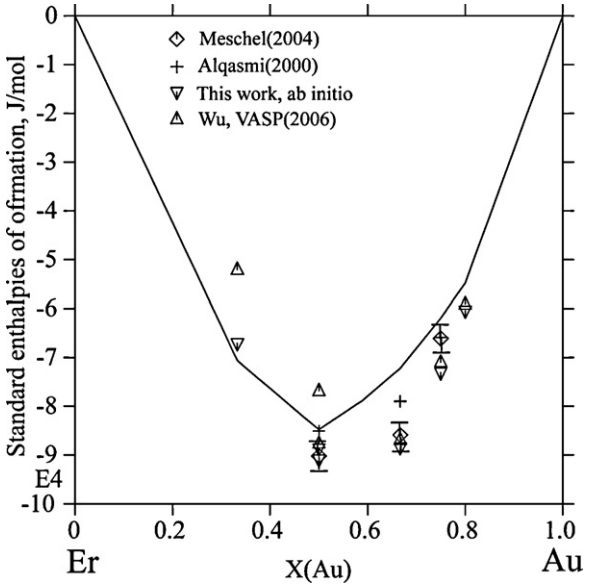

Fig. 2. Enthalpies of formation of in Au–Er binary system at 298 K. Reference states: Au(fcc) and Er(hcp).

Table 2
Thermodynamic parameters of the Au–RE (RE = La and Er) binary systems obtained in this study.

Phase	Thermodynamic parameters
Liquid model: (Au, La)	${}^{0}L^{\mathrm{Liq}}_{\mathrm{Au,La}} = -254446.24 + 6.00025T$
	${}^{1}L^{\mathrm{Liq}}_{\mathrm{Au,La}} = -85046.07 + 2.89377T$
$AuLa_2$ model: $Au_{0.333}La_{0.667}$	$G^{\mathrm{AuLa_2}}_{\mathrm{Au:La}} = -60171.20 + 7.42499T + 0.333\,GH^{\mathrm{SER}}_{\mathrm{Au}} + 0.667\,GH^{\mathrm{SER}}_{\mathrm{La}}$
αAuLa model: $Au_{0.5}La_{0.5}$	$G^{\alpha\mathrm{AuLa}}_{\mathrm{Au:La}} = -82850.00 + 6.10000T + 0.5\,GH^{\mathrm{SER}}_{\mathrm{Au}} + 0.5\,GH^{\mathrm{SER}}_{\mathrm{La}}$
βAuLa model: $Au_{0.5}La_{0.5}$	$G^{\beta\mathrm{AuLa}}_{\mathrm{Au:La}} = -81497.72 + 4.65048T + 0.5\,GH^{\mathrm{SER}}_{\mathrm{Au}} + 0.5\,GH^{\mathrm{SER}}_{\mathrm{La}}$
Au_2La model: $Au_{0.667}La_{0.333}$	$G^{\mathrm{Au_2La}}_{\mathrm{Au:La}} = -77540.39 + 4.63047T + 0.667\,GH^{\mathrm{SER}}_{\mathrm{Au}} + 0.333\,GH^{\mathrm{SER}}_{\mathrm{La}}$
$Au_{51}La_{14}$ model: $Au_{0.785}La_{0.215}$	$G^{\mathrm{Au_{51}La_{14}}}_{\mathrm{Au:La}} = -61127.12 + 2.46619T + 0.785\,GH^{\mathrm{SER}}_{\mathrm{Au}} + 0.215\,GH^{\mathrm{SER}}_{\mathrm{La}}$
Au_6La model: $Au_{0.857}La_{0.143}$	$G^{\mathrm{Au_6La}}_{\mathrm{Au:La}} = -52047.12 + 9.77415T + 0.857\,GH^{\mathrm{SER}}_{\mathrm{Au}} + 0.143\,GH^{\mathrm{SER}}_{\mathrm{La}}$
Liquid model: (Au, Er)	${}^{0}L^{\mathrm{Liq}}_{\mathrm{Au,Er}} = -254942.77 + 12.02066T$
	${}^{1}L^{\mathrm{Liq}}_{\mathrm{Au,Er}} = -76944.03 + 2.98414T$
Fcc model: (Au,Er)	$L^{\mathrm{Fcc}}_{\mathrm{Er}} = 2000 + GH^{\mathrm{SER}}_{\mathrm{Er}}$
	${}^{0}L^{\mathrm{Fcc}}_{\mathrm{Au,Er}} = -159669.49$
	${}^{1}L^{\mathrm{Fcc}}_{\mathrm{Au,Er}} = -138700.88 + 6.47434T$
Hcp model: (Au,Er)	${}^{0}L^{\mathrm{Hcp}}_{\mathrm{Au,Er}} = -110788.94$
$AuEr_2$ model: $Au_{0.333}Er_{0.667}$	$G^{\mathrm{AuEr_2}}_{\mathrm{Au:Er}} = -70674.15 + 12.92470T + 0.333\,GH^{\mathrm{SER}}_{\mathrm{Au}} + 0.667\,GH^{\mathrm{SER}}_{\mathrm{Er}}$
αAuEr model: $Au_{0.5}Er_{0.5}$	$G^{\alpha\mathrm{AuEr_2}}_{\mathrm{Au:Er}} = -84816.96 + 6.10061T + 0.5\,GH^{\mathrm{SER}}_{\mathrm{Au}} + 0.5\,GH^{\mathrm{SER}}_{\mathrm{Er}}$
βAuEr model: $Au_{0.5}Er_{0.5}$	$G^{\beta\mathrm{AuEr_2}}_{\mathrm{Au:Er}} = -76022.80 + 1.45000T + 0.5\,GH^{\mathrm{SER}}_{\mathrm{Au}} + 0.5\,GH^{\mathrm{SER}}_{\mathrm{Er}}$
$Au_{10}Er_7$ model: $Au_{0.588}La_{0.412}$	$G^{\mathrm{Au_{10}Er_7}}_{\mathrm{Au:Er}} = -78899.39 + 4.78648T + 0.588\,GH^{\mathrm{SER}}_{\mathrm{Au}} + 0.412\,GH^{\mathrm{SER}}_{\mathrm{Er}}$
Au_2Er model: $Au_{0.667}Er_{0.333}$	$G^{\mathrm{Au_2Er}}_{\mathrm{Au:Er}} = -72219.36 + 2.85219T + 0.667\,GH^{\mathrm{SER}}_{\mathrm{Au}} + 0.333\,GH^{\mathrm{SER}}_{\mathrm{Er}}$
Au_3Er model: $Au_{0.75}Er_{0.25}$	$G^{\mathrm{Au_3Er}}_{\mathrm{Au:Er}} = -61984.98 + 1.82419T + 0.75\,GH^{\mathrm{SER}}_{\mathrm{Au}} + 0.25\,GH^{\mathrm{SER}}_{\mathrm{Er}}$
Au_4Er model: $Au_{0.8}Er_{0.2}$	$G^{\mathrm{Au_4Er}}_{\mathrm{Au:Er}} = -54809.81 + 3.84705T + 0.8\,GH^{\mathrm{SER}}_{\mathrm{Au}} + 0.2\,GH^{\mathrm{SER}}_{\mathrm{Er}}$

4.2. Thermodynamic assessment

Table 2 lists the parameters evaluated by using the PARROT module in Thermo-Calc software [28] based on the experimental and theoretical data available for the phase diagram. As discussed in the following sections, the present calculations reproduce most of the thermodynamic properties and phase boundary data.

4.2.1. Au–La binary system

The components and temperature of the invariable reactions in the Au–La binary system are listed in Table 3. As illustrated in Fig. 3, a comparison between the assessed phase diagram in this work and the data gained from Ref. [5] was done. There is a good agreement between these two except for the invariable reaction involving Au_2La and $Au_{51}La_{14}$ which has a slightly higher reaction temperature (i.e. 75 K) and is located closer to pure Au (i.e. 4 at.% Au) than reported in Ref. [5] Based on Okamoto and Massalski [29,30] judgment about asymmetry of liquidus curves can be made by comparing the ratio of the width of the two-phase fields on each side of a compound at the same temperature. If the width on one side of the compound is either one half or double that on the other side, the asymmetry may be considered clearly unusual. As for Au_2La phase, the ratio is definitely more two times in the experimentally determined phase diagram, so it should be improved. Hence, in order to fulfill both the liquidus symmetry and the enthalpy of formation of the $AuLa_2$, the eutectic temperature had to be sacrificed. On the other hand, if the liquidus asymmetry of the $AuLa_2$ seen in the experimentally determined phase diagram were reasonable, it indicates some kind of an atom cluster formation in the liquid state. Consequently, the liquid should then be treated with an associate-solution rather than with the regular-solution model. By utilizing associate model, the liquidus can be fitted well with the experimental one, while for the other treatment the fit is not so good. However, according to the criterion of the "associates" the system should have a pronounced "V"-shape enthalpy of mixing curve [31]. According to Fig. 4, no such shape is exhibited. Therefore, the associate-solution is not suitable for the present occasion. With regard to the ascertaining of the Au_6La phase, it was already discussed in Section 2.1. Based on the tem-

Table 3
Invariant reactions in the Au–La binary system.

Reaction	Composition (Au at.%)			T/K	Reference
L ⇔ La(fcc) + $AuLa_2$	16.0	–	–	834	[5]
	16.6	–	–	827	This work
L ⇔ βAuLa	50.0	–		1598	[5]
	–	–		1596	This work
L ⇔ Au_2La	66.7	–		1487	[5]
	–	–		1490	This work
L ⇔ $Au_{51}La_{14}$	78.5	–		1477	[5]
	–	–		1477	This work
L + βAuLa ⇔ $AuLa_2$	24.9	–	–	938	[5]
	24.2	–	–	941	This work
L ⇔ βAuLa + Au_2La	62.7	–	–	1421	[5]
	60.5	–	–	1419	This work
L ⇔ Au_2La + $Au_{51}La_{14}$	69.0	–	–	1327	[5]
	73.1	–	–	1402	This work
L ⇔ Au_6La + Au(fcc)		–	–		[5]
	93.4	–	–	1054	This work
βAuLa ⇔ αAuLa	–	–		933	[5]
	–	–		933	This work
L + $Au_{51}La_{14}$ ⇔ Au_6La					[5]
	88.4	–	–	1175	This work

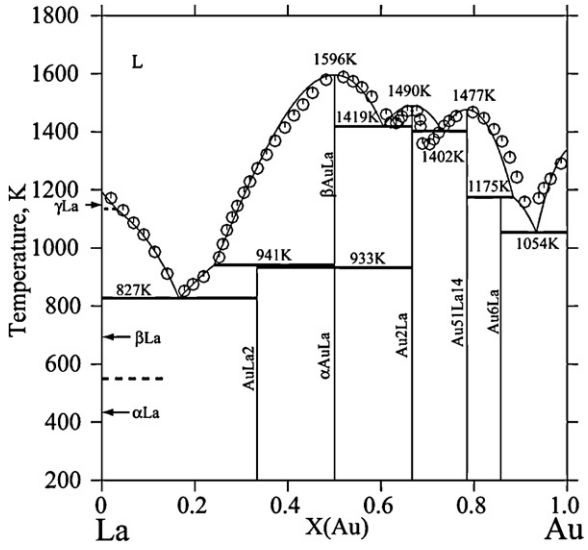

Fig. 3. The calculated phase diagram of the Au–La binary system in comparison with the former work [5].

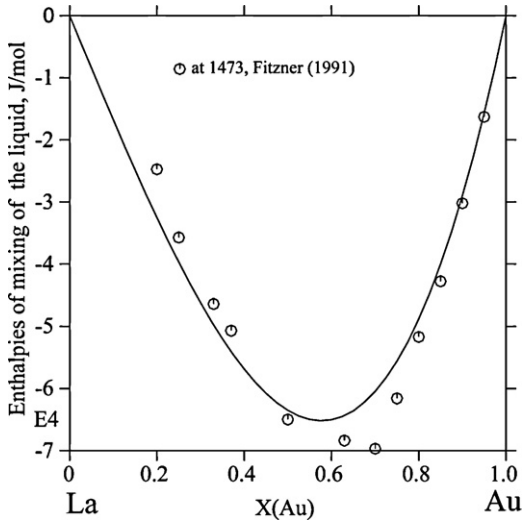

Fig. 4. The calculated enthalpies of mixing of the Au–La alloy at 1473 K in comparison with the experimental data. Reference. states: Au(liquid) and La(liquid).

peratures of the similar invariable reactions in other gold-rear earth system (Table 4 lists those data) and by considering the size ratio as well as the structure of the rear earth elements, temperatures of 1173 K for the $L + Au_{51}La_{14} \leftrightarrow Au_6La$ reaction and 1063 K for the $L \leftrightarrow$ Au(fcc) + Au_6La reaction were employed in this work.

As illustrated in Fig. 4, the measured enthalpies of mixing of the liquid Au–La alloys are reproduced by using the parameters optimized in this work. The standard enthalpies of formation of the intermetallic compounds of the Au–La system were also calculated. As shown in Fig. 1 the experimental data and the results from the ab initio calculations are consistent.

4.2.2. Au–Er binary system

The comparison between the assessed phase diagram and the experimental results is illustrated in Fig. 5. In addition, the composition and temperature of the invariable reactions of the Au–Er binary system are listed in Table 5. The temperature for the allotropic transition (αAuEr ↔ βAuEr) was estimated based on the behavior found in Au–Ho system, i.e. the allotropic transition temperature was taken to be 90 K lower than that of L ↔ βAuEr [6]. This is considered to be justified as both Ho and Er have the same crystal structure, the size ration of the two elements is similar and both of them are translated from CsCl-type to CrB-type during the transition. As for the temperature of the two reactions involving $Au_{10}Er_7$ reported in Ref. [6] these were modified to be 1640 K and 1601 K, respectively. The values 1623 K and 1583 K reported in Ref. [6] were based on the cooling curve of the DTA analysis. The modified values (1640 K and

Table 4
Some invariable reactions of the gold–rear earth binary systems with $Au_{51}X_{14}$ and Au_6X (X = rear earth elements).

Reaction	T/K	Reference
$L + Au_{51}Pr_{14} \Leftrightarrow Au_6Pr$	1173	[5]
$L \Leftrightarrow Au_6Pr$ + Au(fcc)	1063	[5]
$L + Au_{51}Pm_{14} \Leftrightarrow Au_6Pm$	1180	[5]
$L \Leftrightarrow Au_6Pm$ + Au(fcc)	1104	[5]
$L + Au_{51}Nd_{14} \Leftrightarrow Au_6Nd$	1116	[5]
$L \Leftrightarrow Au_6Nd$ + Au(fcc)	1069	[5]
$L + Au_{51}Sm_{14} \Leftrightarrow Au_6Sm$	1073	[5]
$L \Leftrightarrow Au_6Sm$ + Au(fcc)	1043	[5]
$L + Au_{51}Dy_{14} \Leftrightarrow Au_6Dy$	1118	[5]
$L \Leftrightarrow Au_6Dy$ + Au(fcc)	1081	[5]
$L + Au_{51}Gd_{14} \Leftrightarrow Au_6Gd$	–	[5]
$L \Leftrightarrow Au_6Gd$ + Au(fcc)	1082	[5]
$L + Au_{51}Tb_{14} \Leftrightarrow Au_6Tb$	1130	[5]
$L \Leftrightarrow Au_6Tb$ + Au(fcc)	1071	[5]

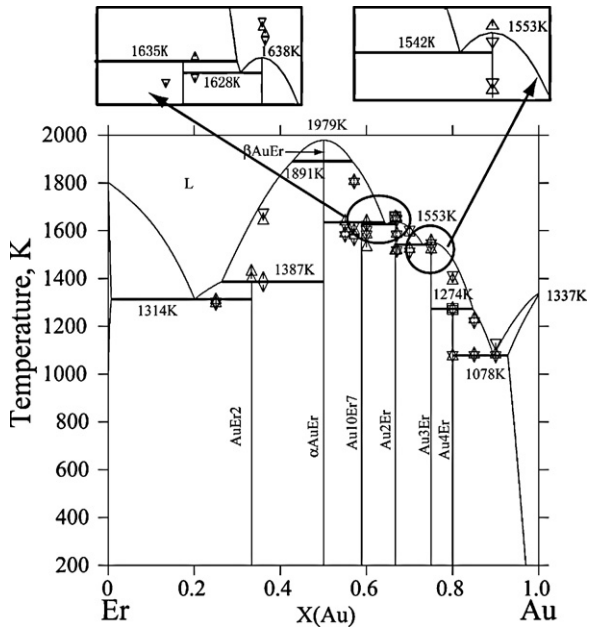

Fig. 5. The calculated phase diagram of Au–Er binary system in comparison with the experimental data [6].

1601 K) used here as the reference values for the calculated values (1635 K and 1628 K) were obtained by considering both the heating and the cooling curves in [6]. This way the problems related to the possible strong undercooling [6] can be minimized. As shown in the figure and the table, the good agreement was achieved except for the eutectic reactions and the congruent melting point. This can be explained as follows: Okamoto and Massalski [32] indicated that if the curvature of the liquidus of a given compound is very sharp in comparison with those of the neighboring compounds, it will not be stable at low temperatures [32]. However, as there is no evidence that the Au_2Er phase will decompose at low temperatures, the existed liquidus should be adjusted to be flatter. Moreover, fitting of the experimentally measured enthalpy of formation of Au_2Er, the optimization work can only be achieved by this way.

Table 5
Invariant reactions in the Au–Er binary system.

Reaction	Composition (at.%Au)			T/K	Reference
$L \Leftrightarrow Er(hcp) + AuEr_2$	24.0	<0.1	–	1303	[6]
	20.0	<0.1	–	1314	This work
$L + \alpha AuEr \Leftrightarrow AuEr_2$	30.0	–	–	1393	[6]
	26.4	–	–	1387	This work
$L \Leftrightarrow \beta AuEr$	50.0	–		1983	[6]
	–	–		1979	This work
$\beta AuEr \Leftrightarrow \alpha AuEr$	50.0	–		1893	[6]
	–	–		1891	This work
$L + \alpha AuEr \Leftrightarrow Au_{10}Er_7$	60.0	–	–	1623	[6]
				1640	Modified from [6]
	64.2	–	–	1635	This work
$L \Leftrightarrow Au_2Er + Au_{10}Er_7$	62.5	–	–	1583	[6]
				1601	Modified from [6]
	64.6	–	–	1628	This work
$L \Leftrightarrow Au_2Er$	66.7	–		1658	[6]
	–	–		1638	This work
$L \Leftrightarrow Au_2Er + Au_3Er$	73.0	–	–	1528	[6]
	73.1	–	–	1542	This work
$L \Leftrightarrow Au_3Er$	75.0	–		1558	[6]
	–	–		1553	This work
$L + Au_3Er \Leftrightarrow Au_4Er$	82.5	–	–	1273	[6]
	84.7	–	–	1274	This work
$L \Leftrightarrow Au_4Er$ + Au(fcc)	89.0	–	94.5	1078	[6]
		–	94.3	1085	[11]
	89.5		92.9	1078	This work

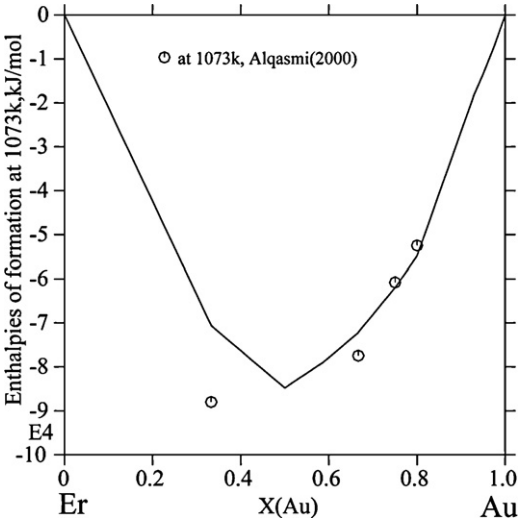

Fig. 6. The calculated enthalpies of formation of the Au–Er alloy at 1073 K. Reference states: Au(fcc) and Er(hcp).

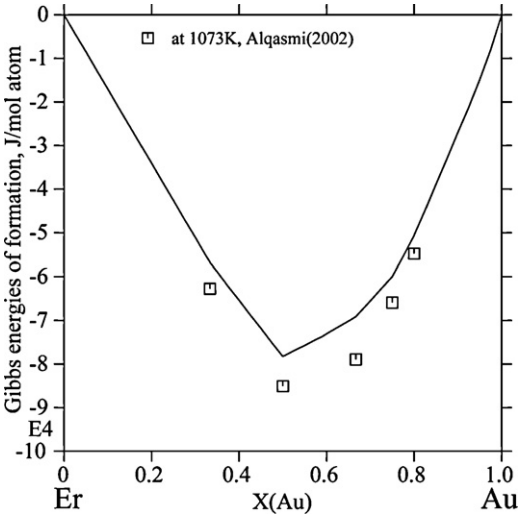

Fig. 7. Gibbs energies of formation of the Au–Er alloy at 1073 K in comparison with experimental data. Reference states: Au(fcc) and Er(hcp).

As illustrated in Fig. 6, the measured enthalpies of formation of the Au–Er alloys at 1073 K are relatively well reproduced by using the optimized parameters. The standard enthalpy of formation of the intermetallic compounds of the Au–La system were also calculated (Fig. 2). Comparison between the experimental data and ab initio calculations shows that the results are consistent. In addition, the Gibbs energies of formation at 1073 K are also well in line with the results from the literature [19] (Fig. 7).

5. Conclusions

With the help of the ab initio calculations, phase relations in the two Au–RE binary systems (Au–La and Au–Er) have been thermodynamically assessed by utilizing the CALPHAD method. A set of thermodynamic parameters describing various phases in these systems have been obtained which can reliably reproduce most of the experimental information. Several issues, which have been unclear in the past, were resolved during the present optimization. These results provide a good starting point for the assessment of the important ternary Au–RE–Sn systems.

Acknowledgements

One of the authors, H.S. Liu, thanks for the financial support from National Natural Science Foundation of China (Grant No. 50671122). Special acknowledgements are given to Dr. Ligang Zhang for illuminating discussion.

References

[1] H.S. Chen, J.W. Yoon, B.I. Noh, J.M. Koo, J.W. Kim, H.J. Lee, S.B. Jung, Microelectron. Reliab. 48 (11–12) (2008) 1857–1863.
[2] Z.G. Chen, Y.W. Shi, Z.D. Xia, Y.F. Yan, J. Electron. Mater. 31 (10) (2002) 1122–1128.
[3] D.Q. Yu, J. Zhao, L. Wang, J. Alloys Compd. 376 (1–2) (2004) 170–175.
[4] W. Xiao, Y.W. Shi, G. Xu, R. Ren, F. Guo, Z.D. Xia, Y.P. Lei, J. Alloys Compd. 472 (1–2) (2009) 198–202.
[5] T.B. Massalski, Binary Alloy Phase Diagrams, ASM International, OH, Metals Park, 1990.
[6] A. Saccone, D. Macci, S. Delfino, R. Ferro, Intermetallics 10 (9) (2002) 903–913.
[7] L. Kaufman, H. Bernstein, Computer Calculation of Phase Diagrams-with Special Reference to Refractory Metals, Academic Press, New York, 1970.
[8] G. Kresse, J. Furthmüller, Phys. Rev. B 54 (16) (1996) 11169–11186.
[9] G. Kresse, J. Furthmüller, Comp. Mater. Sci. 6 (1) (1996) 15–50.
[10] G. Canneri, Metall. Ital. 23 (1931) 803–823.
[11] P.E. Rider, K.A. Gschneidner, O.D. McMasters, Trans. Metall. AIME 233 (1965) 1488–1496.
[12] O.D. McMasters, K.A. Gschneidner Jr., G. Bruzzone, A. Palenzona, J. Less-Comm. Met. 25 (2) (1971) 135–160.
[13] S. Steeb, E. Gebhardt, H. Reule, Monatsh. Chem. Mon. 103 (3) (1972) 716–735.
[14] J.M. Moreau, E. Parthe, Acta Crystall. B: Struct. 30 (7) (1974) 1743–1748.
[15] W.L. Johnson, S.J. Poon, P. Duwez, Phys. Rev. B 11 (1) (1975) 150–154.
[16] K. Fitzner, W.G. Jung, O.J. Kleppa, Metall. Mater. Trans. A 22 (5) (1991) 1103–1111.
[17] S.V. Meschel, O.J. Kleppa, J. Alloys Compd. 363 (2004) 237–242.
[18] V. Sadagopan, B.C. Giessen, N.J. Grant, J. Less-Comm. Met. 14 (1968) 279–290.
[19] R.A. Alqasmi, H.J. Schaller, J. Alloys Compd. 305 (1–2) (2000) 183–187.
[20] Y. Wu, W. Hu, S. Han, J. Alloys Compd. 420 (1–2) (2006) 83–93.
[21] P.E. Blöchl, Phys. Rev. B 50 (24) (1994) 17953–17979.
[22] G. Kresse, J. Joubert, Phys. Rev. B 59 (1999) 1758–1775.
[23] J.P. Perdew, J.A. Chevary, S.H. Vosko, K.A. Jackson, M.R. Pederson, D.J. Singh, C. Fiolhais, Phys. Rev. B 46 (11) (1992) 6671–6687.
[24] J.P. Perdew, Y. Wang, Phys. Rev. B 45 (23) (1992) 13244–13249.
[25] H.J. Monkhorst, J.D. Pack, Phys. Rev. B 13 (12) (1976) 5188–5192.
[26] M. Methfessel, A.T. Paxton, Phys. Rev. B 40 (6) (1989) 3616–3621.
[27] A.T. Dinsdale, Calphad 15 (4) (1991) 317–425.
[28] J.O. Andersson, T. Helander, L. Hglund, P. Shi, B. Sundman, Calphad 26 (2) (2002) 273–312.
[29] H. Okamoto, T.B. Massalski, J. Phase Equilib. 14 (3) (1993) 316–335.
[30] H. Okamoto, T.B. Massalski, J. Phase Equilib. 15 (5) (1994) 500–521.
[31] H.L. Lukas, S.G. Fries, B. Sundman, Computational Thermodynamics the Calphad Method, Cambridge University, New York, 2007.
[32] H. Okamoto, T.B. Massalski, J. Phase Equilib. 12 (2) (1991) 148–168.